IJAMMP

Predictive Maintenance of a Centrifugal Pump Using Vibration Analysis

Zambri bin Abdul Halim *, Mohamad Fauzi Bin Abu Bakar , Fakhrul Azman Bin Mohamed and Azizi Bin Mat Shariff

RESEARCH ARTICLE

ARTICLE INFO

Keywords:

Predictive maintenance;
Centrifugal pump;
Vibration analysis;
Bearing fault diagnosis;
Order analysis

Article History

*Received:*24 October 2025
*Revised:*19 February 2026
*Accepted:*28 February 2026
Published:

Centrifugal pumps are critical components in industrial systems where bearing failures may result in significant downtime and economic losses. This study investigates the vibration condition of a 450 kW centrifugal pump using condition-based predictive maintenance techniques. Vibration data were acquired from Pump Bearing #4 (Free End, 6321) under steady-state operation and analyzed using Time Waveform (TWF) and Fast Fourier Transform (FFT) spectrum analysis. The calculated bearing characteristic frequencies—Fundamental Train Frequency (FTF), Ball Pass Frequency Outer Race (BPFO), Ball Pass Frequency Inner Race (BPFI), and Ball Spin Frequency (BSF)—were compared with spectral peaks expressed in order analysis. Results indicate dominant harmonics between 21× and 25× orders corresponding to BPFI, confirming advanced inner race spalling. Sideband modulation and repetitive impact patterns further support the diagnosis. Physical inspection after disassembly validated the presence of localized inner and outer race damage. The findings demonstrate that vibration-based condition monitoring is effective for early fault detection and fault progression assessment in high-power centrifugal pump systems.

1.Introduction

Centrifugal pumps play a critical role in industrial sectors including power generation, petrochemical processing, and water treatment, where their reliability directly affects plant availability and operational continuity. As highlighted by Singh and Saini (2023), the performance stability of centrifugal pumps is closely linked to effective fault detection strategies. In practice, unexpected pump failures often lead to production downtime, increased energy consumption, and elevated maintenance costs, with bearing degradation identified as a major contributor to rotating machinery breakdown (Zhao et al., 2020). Traditional preventive and corrective maintenance strategies are frequently insufficient for detecting incipient bearing defects before severe damage develops.

Consequently, predictive maintenance approaches—particularly vibration-based condition monitoring—have gained widespread acceptance in industrial diagnostics (Lei et al., 2021). Randall and Antoni (2020) emphasized that frequency-domain analysis enables the identification of characteristic defect frequencies associated with specific bearing fault mechanisms.

Department of Mechanical & Production Engineering Technology, Mechatronic Division, Japan-Malaysia Technical Institute (JMTI), 14100, Simpang Ampat, Penang, Malaysia

Corresponding author*: zambri@jtm.gov.my

More recent advancements in signal processing further enhance diagnostic sensitivity. Techniques such as envelope spectrum analysis, spectral kurtosis, and order tracking have been shown to improve early-stage defect detectability, especially under noisy or variable-speed operating conditions (Kumar & Sharma, 2024; Zhang et al., 2022). These developments reinforce the importance of combining classical frequency analysis with advanced processing methods.

In this context, the present study investigates the vibration behaviour of Pump Bearing #4 (Free End, 6321) in a 450-kW centrifugal pump system. The analysis focuses on frequency-domain characteristics and comparative assessment within the drive train. Particular attention is given to the identification of key bearing fault frequencies—including Ball Pass Frequency Inner race (BPFI), Ball Pass Frequency Outer race (BPFO), Ball Spin Frequency (BSF), and Fundamental Train Frequency (FTF)—to evaluate fault severity and progression.

2. Literature Review

The characteristic fault frequencies of a rolling element bearing are governed by its geometric parameters, including the number of rolling elements, pitch diameter, rolling element diameter, contact angle, and shaft rotational speed. These parameters determine the location of defect-related spectral components and constitute the theoretical

foundation of vibration-based bearing diagnostics. As discussed by Randall and Antoni (2020), the analytical formulation of bearing characteristic frequencies enables precise identification of defect mechanisms in the frequency domain.

Recent studies further confirm that characteristic defect frequencies—such as Ball Pass Frequency of the Inner Race (BPFI), Ball Pass Frequency of the Outer Race (BPFO), Ball Spin Frequency (BSF), and Fundamental Train Frequency (FTF) are remain widely applied in modern industrial condition monitoring systems for fault localization and severity assessment (Zhang et al., 2022).

$$\mathrm{BPFI} = \frac{Z}{2} S \left[1 + \left(\frac{B_d}{P_d}\right) \cos\theta\right] \quad (1)$$

$$\mathrm{BPFO} = \frac{Z}{2} S \left[1 - \left(\frac{B_d}{P_d}\right) \cos\theta\right] \quad (2)$$

$$\mathrm{BSF} = \frac{P_d}{2B_d} S \left[1 - \left(\frac{B_d}{P_d}\right)^2 \cos^2\theta\right] \quad (3)$$

$$\mathrm{FTF} = \frac{1}{2} S \left[1 - \left(\frac{B_d}{P_d}\right) \cos\theta\right] \quad (4)$$

Where:

- S = rotational speed in revolutions per second.
- Z = number of rolling elements.
- B_d = ball or roller diameter, mm.
- P_d = bearing pitch diameter, mm.
- θ = contact angle.

Characteristic fault frequencies provide a reliable basis for diagnosing rolling element bearing defects. Outer race faults typically produce dominant BPFO components and harmonics, while inner race defects are characterized by strong BPFI responses accompanied by sideband modulation spaced at the shaft rotational frequency (Lei et al., 2021; Singh & Saini, 2023). Rolling element and cage defects are generally associated with BSF and FTF components, respectively, reflecting their distinct kinematic behavior (Randall & Antoni, 2020).

Recent advancements highlight that integrating these theoretical fault frequencies with envelope analysis, spectral kurtosis, and order tracking significantly improves fault localization accuracy, particularly under variable-speed and noisy operating conditions (Kumar & Sharma, 2024; Zhang et al., 2022; Zhao et al., 2020).

3. Measurement Setup and Methodology

The vibration measurement configuration for the centrifugal pump system is summarized in Table 1. The test was performed on a 450 kW centrifugal pump operating at 989 RPM (≈ 16.48 Hz), equipped with a closed six-blade impeller and a direct motor–pump coupling. The bearing under investigation was the pump free-end bearing (Location #4), identified as a 6321 deep-groove ball bearing designed to support both radial and axial loads. Vibration-based diagnostics of centrifugal pump bearings under steady-state conditions remain a widely accepted approach for reliable spectral fault identification (Lei et al., 2021; Singh & Saini, 2023). As emphasized by Zhao et al. (2020) and Kumar and Sharma (2024), appropriate sensor placement and multi-directional measurements are critical to improving diagnostic sensitivity. In this study, a tri-axial accelerometer was mounted vertically on the pump housing to capture vibration responses transmitted through the bearing structure, consistent with modern condition monitoring frameworks. All measurements were acquired under stable operating conditions to ensure consistency in frequency-domain analysis and accurate identification of characteristic defect frequencies. The reliability of steady-state spectral interpretation has been extensively discussed in the literature, particularly in relation to harmonic identification and fault localization (Randall & Antoni, 2020; Zhang et al., 2022).

Table 1. Measurement setup for centrifugal pump system.

Parameter	Specification
Motor power	450 KW
Operating Speed	989 RPM (~16.48 Hz)
Pump Type	Centrifugal (closed impeller, six blades)
Coupling	Motor–pump direct coupling
Bearing Inspected	6321 deep groove ball bearing
Location	pump free end (Location #4)

Vibration measurements were collected in axial, tangential, and radial directions using the Fluke 810 diagnostic analyzer. The calculated fault frequencies for the 6321 bearing are summarized in Table 2, with order values of FTF = 0.38, BPFO = 3.08, BPFI = 4.92, and BSF = 2.05.

Table 2 summarizes the key fault frequency formulas used in this study. The Fundamental Train Frequency (FTF) represents the cage rotational frequency and is primarily used to detect cage-related faults. The Ball Pass Frequency Outer Race (BPFO) and Ball Pass Frequency Inner Race (BPFI) correspond to defects occurring on the outer and inner raceways, respectively, while the Ball Spin Frequency (BSF) represents the rotation of the individual rolling elements, which is associated with ball surface damage. The calculated theoretical order values for the 6321 bearing were 0.38× for FTF, 3.08× for BPFO, 4.92× for BPFI, and 2.05× for BSF, where "×" indicates multiples of the shaft rotational speed. These order values serve as reference points in the vibration spectrum for identifying characteristic defect peaks.

Table 2 Bearing 6321 fault frequencies.

Fault frequency	Formula	Description	Order value
FTF (Fundamental Train Frequency)	$FTF = \frac{1}{2} f_r \left[1 - \left(\frac{d}{D_p}\right)\cos\theta\right]$	Cage frequency; useful for detecting cage faults.	0.38
BPFO (Ball Pass Frequency, Outer Race)	$BPFO = \frac{Z}{2} f_r \left[1 - \left(\frac{d}{D_p}\right)\cos\theta\right]$	Outer race defect frequency.	3.08
BPFI (Ball Pass Frequency, Inner Race)	$BPFI = \frac{Z}{2} f_r \left[1 + \left(\frac{d}{D_p}\right)\cos\theta\right]$	Inner race defect frequency.	4.92
BSF (Ball Spin Frequency)	$BSF = \frac{D_p}{2d} f_r \left[1 - \left(\frac{d}{D_p}\cos\theta\right)^2\right]$	Ball spin frequency; indicates ball defects.	2.05

Figure 1 shows the vibration measurement setup on the centrifugal pump assembly. A tri-axial accelerometer was mounted on the vertical position of the free-end bearing housing, which supports the pump shaft and accommodates axial and thermal expansion during operation.

Figure 1: Tri-axial acceleration sensor mounted on bearing #4 (Free End, 6321) in vertical direction.

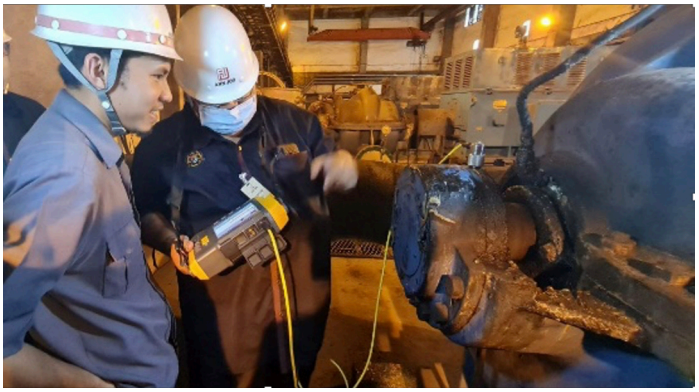

4. Results and Discussion

4.1 Time Waveform (TWF)

Figure 2 shows the time waveform (TWF) signals for both axial and radial directions indicate periodic impact patterns with a fundamental period of approximately 0.062 s, corresponding to the shaft rotational speed of around 16.48 Hz. The axial signal exhibits higher impulsive peaks compared to the radial direction, suggesting stronger thrust or axial loading transmitted through the bearing structure. The presence of repeated impacts in both axes implies localized bearing excitation, possibly due to inner-race or rolling-element surface irregularities that generate vibration responses synchronized with shaft rotation.

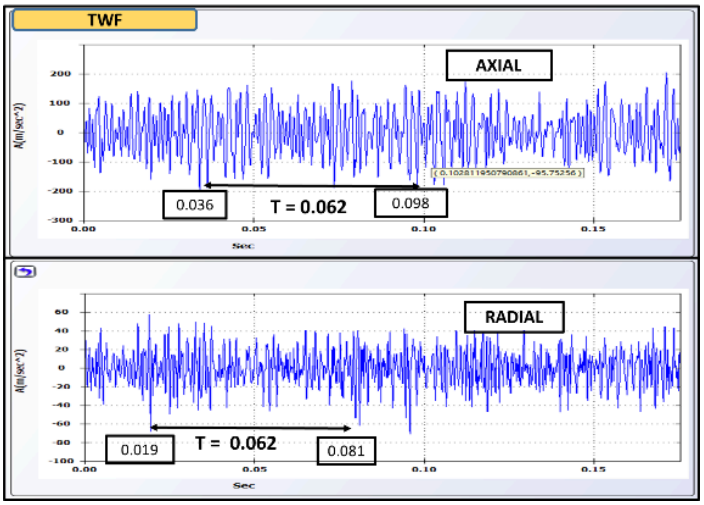

Figure 2: Time waveform (TWF) signals for both axial and radial directions.

4.2 High range spectrum analysis

Figure 3 shows the spectrum shows a dominant peak at 25× order with amplitude ~10.15 mm/s, matching harmonics of BPFI (Ball Pass Frequency Inner race). This indicates advanced inner race fault. The axial direction is most severe because thrust load from the impeller is transmitted through the inner race. Figure 4 shows a strong spectral peak at 21× order with amplitude ~9.17 mm/s. Tangential vibration confirms bearing fault modulation due to spalling. Sidebands around 20× and 22× orders indicate repeated impacts each time rolling elements pass the defect. High tangential amplitude shows the defect is in an advanced stage.

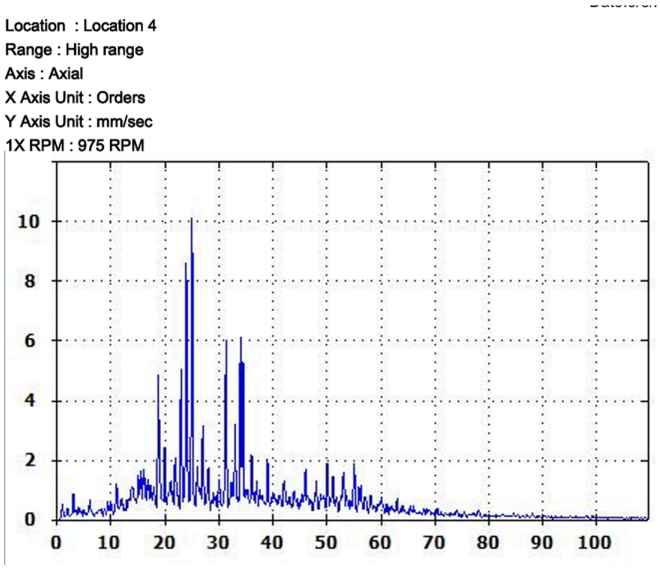

Figure 3. Spectrum Axial (High Range) – Pump Bearing #4 (Free End, 6321).

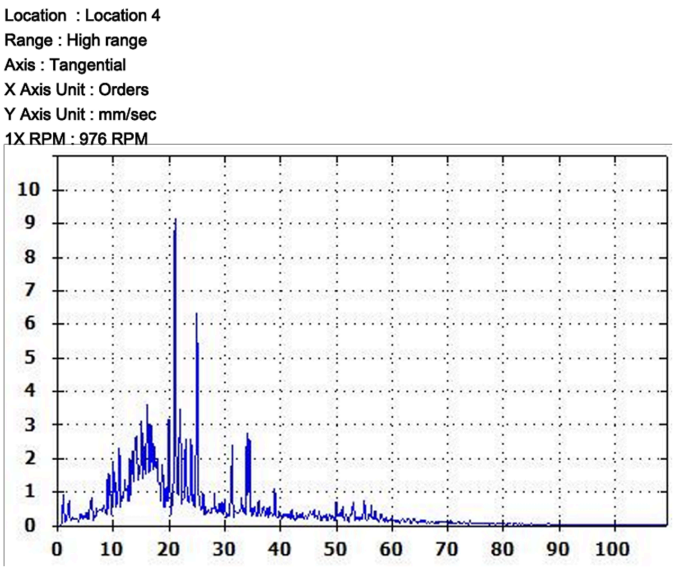

Figure 4: Spectrum Tangential (High Range) – Pump Bearing #4 (Free End, 6321).

Figure 5 shows a zoomed view of the spectral region around the dominant 21× order peak shown in Figure 4. In addition to the principal harmonic at approximately 21×, adjacent spectral components are clearly observed at approximately 20× and 22× orders. The spacing between these peaks is approximately equal to 1× shaft rotational frequency.

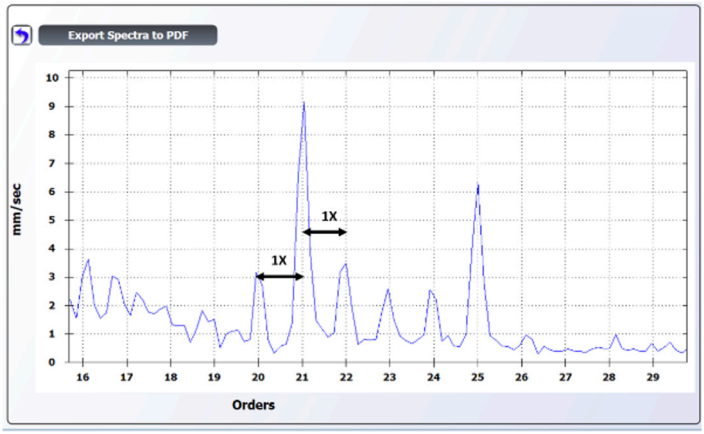

Fig. 5: Enlarged Spectrum from Figure 4 Showing ±1× Sidebands Around the BPFI Harmonic.

Sidebands arise from amplitude modulation, which occurs when a high-frequency defect signal is periodically influenced by a lower-frequency rotating component. In rolling element bearings, a localized defect on the inner race rotates together with the shaft. Each time a rolling element passes over the defect, an impact is generated. However, because the defect itself rotates with the shaft, the impact intensity varies cyclically with shaft rotation. This periodic variation in amplitude produces modulation at the shaft rotational frequency. Such symmetric ±1× spacing indicates amplitude modulation behavior. In rolling element bearings, when a localized inner race defect rotates with the shaft, the impact-induced vibration signal is periodically modulated at shaft rotational frequency.

This produces frequency components of the form:

$$f = f_{\text{fault}} \pm n f_r \tag{5}$$

where f_r is the shaft rotational frequency and n is an integer sideband order.

In the present spectrum, symmetric peaks at approximately 20× and 22× surrounding the dominant 21× component demonstrate clear ±1× spacing. This confirms that the 21× harmonic is modulated by the shaft rotational frequency. Such modulation behavior is widely recognized as a diagnostic signature of inner race defects, as damage on the inner race rotates with the shaft and inherently produces amplitude modulation effects (Lei et al., 2021; Randall & Antoni, 2020).

Figure 6 presents the radial spectrum, which exhibits a lower dominant amplitude of approximately 1.54 mm/s at 25× order but shows broadband excitation extending up to 34× order. This broadband response is characteristic of impact-induced energy exciting structural resonances within the bearing–housing system. Although the radial vibration severity is lower compared to axial and tangential directions, the presence of broadband excitation confirms the propagation of impulsive energy through the housing structure, indicating ongoing fault progression.

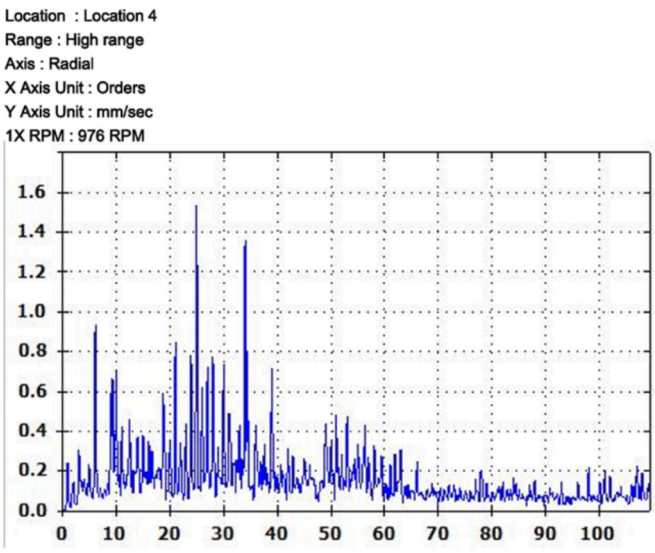

Figure 6: Spectrum Radial (High Range) – Pump Bearing #4 (Free End, 6321).

4.3 Low range spectrum analysis

Figure 7 shows peaks detected at 3.05× (0.86 mm/s) and 6.1× (0.83 mm/s) orders fall within the Ball Spin Frequency (BSF) sideband region, indicating early impact modulation. Although amplitudes are smaller compared to high range, the sideband pattern is an early symptom of inner race defect development. This shows fault initiation before high-order harmonics dominate.

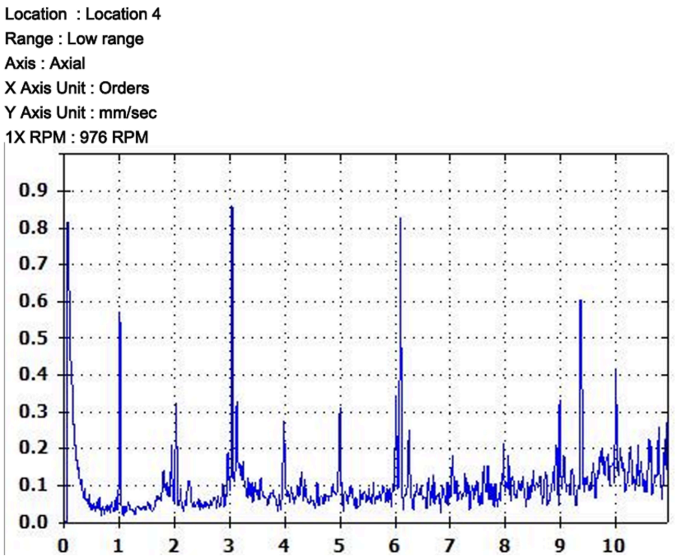

Figure 7. Spectrum Axial (Low Range) – Pump Bearing #4 (Free End, 6321)

Figure 8 shows peaks at 8.84× (1.60 mm/s) and 9.21× (1.45 mm/s) orders align with BPFI (Ball Pass Frequency Inner race). This provides direct evidence of early inner race defect. Sidebands surrounding BPFI confirm repeated rolling element impacts at the defect. Tangential direction is highly sensitive for early-stage detection, making it suitable for long-term trend monitoring.

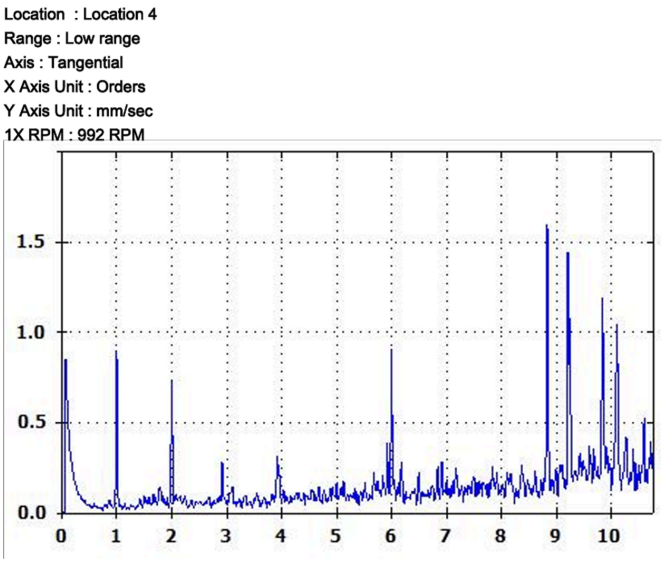

Figure 8: Spectrum Tangential (Low Range) – Pump Bearing #4 (Free End, 6321).

Figure 9 shows a peak around 9.84× order (0.62 mm/s) indicates harmonic/sideband build-up. Although amplitudes are lower than axial/tangential, the radial spectrum confirms that defect energy is spreading. This spectrum acts as secondary evidence supporting inner race fault diagnosis.

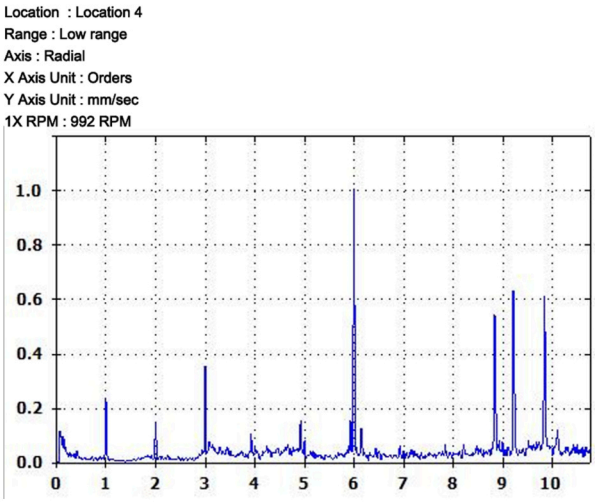

Figure 9. Spectrum Radial (Low Range) – Pump Bearing #4 (Free End, 6321).

Figure 10 shows the physical condition of Pump Bearing #4 (Free End, 6321) after disassembly, confirming the presence of a localized inner race spalling defect. The damage is characterized by a distinct pit and material flaking along the raceway, consistent with surface fatigue failure resulting from repeated rolling contact stress. This type of defect typically develops when localized subsurface cracks propagate to the surface under cyclic loading. The physical evidence aligns with the vibration analysis results, where the BPFI (Ball Pass Frequency of Inner Race) and its harmonics were dominant in both the low- and high-range spectra, indicating progressive inner race degradation. The visual confirmation validates the diagnostic conclusion obtained from the TWF and FFT analyses.

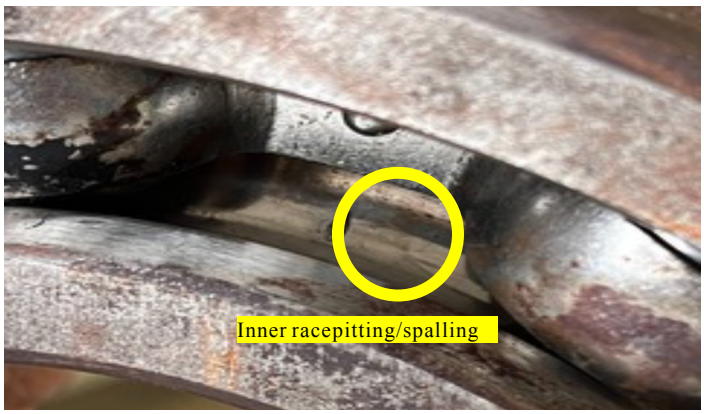

Figure 10. The physical condition of Pump Bearing #4 (Free End, 6321) after disassembly.

5. Conclusion

The time waveform (TWF) and order-based spectral analyses confirm a localized inner race defect in Pump Bearing #4 (Free End, 6321). The repetitive impact impulses, symmetric ±1× sideband spacing, and amplitude modulation behavior provide strong evidence of inner race spalling. The dominant harmonics observed in the 21×–25× order range indicate nonlinear impact excitation and resonance amplification, suggesting that the defect has progressed to an advanced stage.

The combined interpretation of low-range and high-range spectra enables systematic fault progression assessment, where early BPFI-related components evolve into dominant higher-order harmonics as severity increases. From a maintenance perspective, order-based monitoring with sideband verification should be incorporated into routine condition monitoring to support predictive maintenance planning and prevent unplanned failure.

This study was conducted under steady-state operating conditions on a single bearing configuration. Future research should extend the analysis to variable-speed environments and integrate advanced signal processing techniques, such as envelope analysis and spectral kurtosis, to enhance early fault detection and diagnostic reliability.

References

Kumar, S., & Sharma, R. (2024). Multi-sensor data fusion for intelligent predictive maintenance of rotating machinery. Sensors, 24(3).

Lei, Y., Li, N., Guo, L., Li, N., Yan, T., & Lin, J. (2021). Machinery health prognostics: A systematic review from data acquisition to RUL prediction. Mechanical Systems and Signal Processing, 104, 799–834.

Randall, R. B., & Antoni, J. (2020). Rolling element bearing diagnostics—Recent advances. Mechanical Systems and Signal Processing, 145.

Singh, A., & Saini, P. K. (2023). Vibration-based fault diagnosis of centrifugal pumps: A review. Journal of Fluids Engineering, 145(4).

Zhang, X., Qin, Q., & Wang, H. (2022). Order tracking and time–frequency analysis for bearing fault diagnosis under variable speed conditions. Journal of Vibration and Control, 28(5–6), 712–728.

Zhao, R., Yan, R., Chen, Z., Mao, K., & Shen, F. (2020). Deep learning and vibration-based predictive maintenance: A review. IEEE Access, 8, 131363–131378.